

D. A. Durston* and D. B. Smeltzer†
 NASA Ames Research Center, Moffett Field, California

Abstract

Aerodynamic force and inlet-pressure data were obtained for 9.5% force and pressure models of a V/STOL fighter/attack aircraft configuration with top-mounted twin inlets. Data are presented from tests conducted in the Ames Unitary Wind Tunnels at Mach numbers of 0.6, 0.9, and 1.2 at angles of attack up to 27° and angles of sideslip up to 12°. Trimmed aerodynamic characteristics and inlet performance were compared for three different leading-edge extension (LEX) configurations. The effects of wing leading- and trailing-edge flaps on the inlet were also determined. Maneuver performance was calculated from combined force and inlet-pressure data. The largest of the three LEX sizes tested gave the best airplane maneuver performance. Wing flap deflections improved inlet recovery at all Mach numbers.

Nomenclature

AR	= aspect ratio
C_{D_T}	= trimmed drag coefficient
C_{L_T}	= trimmed lift coefficient
C_T/C_R	= taper ratio, wing tip/root chord
h	= altitude, m (ft)
LEX	= wing leading-edge extension
$(L/D)_{T_{max}}$	= maximum trimmed-lift-to-drag-ratio
$(L/D)_{T_{cruise}}$	= trimmed-lift-to-drag ratio at cruise angles of attack
M	= Mach number
n_z	= load factor
P_s	= specific excess power, m/sec (ft/sec)
α_T	= trimmed angle of attack, deg
β	= angle of sideslip, deg
Λ_{LE}	= wing leading-edge sweep angle, deg

Introduction

Inlet integration studies¹ and aerodynamic technology studies² indicate that fighter/attack aircraft configurations with top-mounted inlets have significant potential advantages over configurations with more conventionally mounted inlets.

Among these advantages are reduced ingestion of debris, reduced radar return to ground radars, and better weapons integration on the lower fuselage. However, the studies of Ref. 2 also identified aerodynamic uncertainties and potential inlet problem areas. Aerodynamic uncertainties relating to inlet location included a slight increase in wave drag with increasing supersonic Mach number and a possible adverse effect on minimum drag because of inlet spillage. Potential inlet problem areas included the ingestion of distorted flow and/or low-energy boundary layers at high angles of attack and/or moderate sideslip angles.

The top-mounted twin-inlet configuration identified in Ref. 2 was based on a detailed aerodynamic analysis by Northrop Corporation³ in a program jointly sponsored by Ames Research Center and the David Taylor Naval Ship Research and Development Center. An aerodynamic force model of this configuration was constructed and tested in the high-speed wind tunnels at Ames. Wing leading-edge extensions (LEXs) on the model produced vortices to lessen the low energy boundary layer flow in front of the inlets. The model had flow-through ducts and limited pressure instrumentation in the inlet throat. Some of the force and pressure results from these tests were reported in Refs. 4 and 5. The model was then modified and more detailed inlet-pressure tests, in which data were taken in the upper fuselage flow field, in the inlet throat, and at the compressor face station, were conducted. Some results from these inlet-pressure tests were reported in Refs. 6-8.

The objective of this paper is to compare the aerodynamic characteristics and inlet performance of the different LEX sizes investigated in the tests mentioned above and to determine the LEX size for best airplane maneuver performance.

Top-Inlet Configuration

Photographs of both models are shown in Fig. 1. The 9.5% scale models are shown in separate installations in the 11- by 11-Foot Transonic Wind Tunnel at Ames Research Center. Orthographic views of the models and their respective instrumentation are presented in Figs. 2 and 3. Figures 1-3 show the models with the largest LEX. Aerodynamic forces were determined from a six-component strain-gage balance in the force model. The inlet model was instrumented at the compressor face of each duct (Fig. 4). This instrumentation consisted of 4 circumferential static pressure taps, 12 total pressure probes, and 6 Kulite dynamic/total pressure transducers. Both models were tested with various wing leading- and trailing-edge flap deflections (Fig. 2) and with three different wing leading-edge extension (LEX) options: large, small, and off (Fig. 5). The large LEX was considered the baseline for both models. The small LEX retained the same shape as the large one but had only 60% of its plan area. LEX-off was simulated by extending the wing leading edge straight to the fuselage.

*Research Scientist, Member AIAA

†Research Scientist

Wind tunnel test data considered in this paper were taken at Mach numbers of 0.6, 0.9, and 1.2, at angles of attack up to 27°, and at angles of sideslip up to 12°. The reference area for all aerodynamic data presented in this paper is the wing area with the wing leading- and trailing-edges extended to the fuselage centerline. Thus, changes in LEX area are not reflected in the aerodynamic coefficients.

Results

Trimmed aerodynamic characteristics from the force model tests are presented first for the three LEX sizes. Inlet pressure recoveries and distortion from the inlet-pressure model tests are analyzed next for all three LEX sizes and for two different wing leading- and trailing-edge flap deflections. Finally, the force and inlet pressure results are combined into a maneuver performance summary to determine the effects of LEX size.

Trimmed Aerodynamic Characteristics

Trimmed lift and drag curves are presented for Mach numbers of 0.6 (Fig. 6), 0.9 (Fig. 7), and 1.2 (Fig. 8). The model was trimmed for minimum drag using both the leading- and trailing-edge wing flaps. Insufficient test data were taken to include the small LEX or LEX-off results at Mach 1.2. The subsonic drag polars (Figs. 6 and 7) show that the large LEX has the least overall drag of the three LEX options. This LEX also produces the highest lift curve slopes at these Mach numbers, though the maximum trimmed lift ($C_{L_T} = 1.15$) is less than that of the small LEX ($C_{L_T} = 1.25$) at Mach 0.6. The maximum trimmed lift for both the large and small LEXs is identical at Mach 0.9 ($C_{L_T} = 1.25$).

Figures 6 and 7 show that the model can be trimmed to higher angles of attack with decreasing LEX size. Smaller LEX sizes produce less nose-up pitching moment which must be overcome by the wing flaps. Larger LEX sizes would require more powerful wing trailing-edge flaps.

The data at Mach 1.2 illustrate that a relatively high trimmed lift coefficient ($C_{L_T} = 1.20$) can be achieved at low supersonic speeds.

Maximum and cruise trimmed lift-to-drag ratio summaries are presented in Fig. 9 for the three LEX options. The large LEX maintains the highest maximum $(L/D)_T$ (Fig. 9a) of the three options through the subsonic Mach number range, with an exception at Mach 0.2, where the values of $(L/D)_{T_{max}}$ are the same for all three LEX options. The cruise lift-to-drag ratios (Fig. 9b) were computed for an altitude of 9144 m (30,000 ft), using a gross weight of 11,975 kg (26,400 lb) (obtained from Ref. 3). The curves show that the large LEX has the best cruise lift-to-drag ratios up to Mach 0.9. The cruise $(L/D)_T$ of the small LEX at this Mach number is the same as that of the large LEX. The LEX-off option has substantially lower cruise values of $(L/D)_T$ than either of the two LEX's.

Inlet Performance

Average inlet pressure recoveries and distortion values are shown in Fig. 10 for the three LEX

configurations at Mach numbers of 0.6, 0.9, and 1.2. Average pressure recovery per inlet is defined as the area-weighted average of the compressor face rake total pressures divided by the wind tunnel free stream total pressure. The area-weighting refers to a small area around each probe of the rake resulting from the subdivision of the total compressor face area. Distortion is defined as the maximum total pressure difference between probes divided by the average pressure recovery. These results are for undeflected leading- and trailing-edge flaps (see subsequent text for flap deflection effects on inlet performance). At all Mach numbers, both the large and small LEXs produce comparable performance. The small LEX produces slightly better performance (higher recoveries and lower distortions) at low-to-moderate angles of attack, and the large LEX is better at the higher angles. This may be attributed to a more rearward vortex breakdown point with the larger LEX. A water tunnel investigation⁹ demonstrated this characteristic for angles of attack below 30°. The LEX-off configuration is clearly inferior to the two LEX configurations at all Mach numbers, particularly at moderate-to-high angles of attack.

The data in Fig. 10 are for a sideslip angle of 0°, but fighter/attack aircraft often operate at nonzero sideslip angles. Figure 11 presents distortion-limited operating envelopes at nonzero angles of attack and sideslip. The distortion is less than or equal to 20% in the crosshatched regions, and this is assumed to be a representative engine operating limit. The windward and leeward inlets are indicated in figure 11; at positive sideslip angles, the right inlet is windward and the left inlet is leeward.

Data are shown for all three LEX configurations at Mach numbers of 0.6, 0.9, and 1.2. Distortion limits at high sideslip angles for the leeward inlet with the small LEX at Mach 0.9 and 1.2 could not be determined because of insufficient test data.

The top row of figures in Fig. 11 shows the LEX-off case with regions where the distortion exceeds 20% (the regions that are not crosshatched). At Mach 0.6 these regions are small, but at Mach 0.9 they become large enough to cover most of the windward inlet side at sideslip angles greater than 2°. At Mach 1.2, the region covers the entire windward side, except for the lowest and highest sideslip angles at angles of attack below 13°. Increasing the LEX size greatly reduces these regions. At subsonic Mach numbers, the large LEX has very small regions in which the distortion exceeds 20%, but at Mach 1.2 those regions are of moderate size. For sideslip angles below 5° and at all angles of attack tested, the large LEX can provide a flow field in which the inlet distortion is less than 20% at the three test Mach numbers.

The windward inlet typically has the largest regions of high distortion. For side-mounted inlets, the opposite is typical: that is, the leeward inlet has the highest distortion.

The effect of leading- and trailing-edge flaps on inlet recovery and distortion at Mach numbers of 0.6, 0.9, and 1.2 is shown in Fig. 12. Data are presented for both sets of flaps undeflected and at

30° for zero sideslip angle. Deflecting the flaps increases the pressure recovery up to 2% for the entire angle of attack range tested and for all three Mach numbers. Distortion is reduced with flap deflection mostly at the lower angles of attack; there are small increases at the higher angles. These results indicate that flap deflections improve inlet pressure recovery slightly for this configuration without adversely affecting distortion.

Airplane Maneuver Performance

Figure 13 shows specific excess power (P_s) as a function of load factor (n_z) for all three LEX options at $M = 0.6$ and 0.9 and for the large LEX at $M = 1.2$. Calculations were made for an altitude of 9144 m (30,000 ft). The specific excess power is a function of thrust minus drag and is approximately equivalent to the climb rate and the longitudinal acceleration. Correspondingly, normal load factor is equivalent to turn rate and lateral acceleration. The engine thrust and the estimated engine losses in the P_s calculations were those used in Ref. 3, with a correction included for the effects of inlet pressure recovery on thrust. Measured inlet pressure recoveries were used to adjust the computed thrust levels at the correct angles of attack. The flap deflection effects on pressure recovery were not included for some load factors because of insufficient test data. Specifically, they were not included for load factors above 2 and 3 for the small LEX and for LEX-off respectively at $M = 0.6$; and for load factors above 5 and 7 for the small LEX and for LEX-off respectively at $M = 0.9$. The pressure recoveries at these conditions were conservatively estimated to be those values at zero-flap-deflection angles (recall that recoveries were found to increase with increasing flap deflection for the large LEX). Distortion under 20% was assumed to have no effect on thrust, and for the angles and conditions represented in Fig. 13 the distortion never exceeded 20%.

The mass flow in the flow-through ducts was scaled according to the airplane design engine airflow. A structural design limit of 8 g's is shown for reference.

The combined force and pressure recovery results from the preceding sections show that the large LEX has an advantage in maneuver performance over the other LEX options at Mach numbers of 0.6 and 0.9. The only disadvantage of this LEX is at $M = 0.6$ where the inability to trim at high angles of attack limits the load factor to about 3.5; with the small LEX the maximum load factor is about 3.75. At Mach 1.2, the large LEX provides more specific excess power than at Mach 0.6 or 0.9 over the entire range of load factors.

Conclusions

Aerodynamic and inlet performance data have been analyzed for a top-mounted inlet fighter/attack aircraft configuration. The configuration variables investigated were LEX size and leading- and trailing-edge flap deflections. The results are summarized as follows:

1) Of the three LEX options, the large LEX produced the best trimmed lift and drag.

2) The large and small LEXs gave essentially the same inlet pressure recoveries, and the LEX-off gave much lower recoveries at high angles of attack.

3) Increasing LEX size greatly reduces distortion at moderate sideslip angles, especially at higher Mach numbers.

4) Wing leading- and trailing-edge flap deflections improved inlet recoveries slightly without adversely affecting distortion.

5) The large LEX gave the best overall maneuver performance.

References

¹Williams, T. L. and Hunt, B. L., "A Comparative Assessment of Top-Mounted and Conventional Inlet/Airframe Integrations," Conference Publication 2162, Part 2, Tactical Aircraft Research and Technology Conference, NASA Langley Research Center, Hampton, Va., Oct. 21-23, 1980.

²Nelms, W. P., "Studies of Aerodynamic Technology for V/STOL Fighter/Attack Aircraft," AIAA Paper 78-1511, AIAA Aircraft Systems and Technology Conference, Los Angeles, Calif., 1978.

³Gerhardt, H. A. et al., "Study of Aerodynamic Technology for V/STOL Fighter/Attack Aircraft - Vertical Attitude Concept," NASA CR-152131, 1978.

⁴Nelms, W. P. and Durston, D. A., "Preliminary Aerodynamic Characteristics of Several Advanced V/STOL Fighter/Attack Aircraft Concepts," SAE Paper 801178, SAE Aerospace Congress and Exposition, Los Angeles, Calif., Oct. 13-16, 1980.

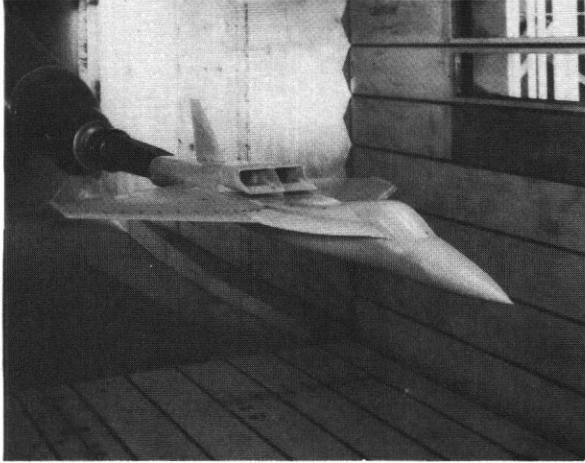
⁵Durston, D. A. and Smith, S. C., "Lift-Enhancing Surfaces on Several Advanced V/STOL Fighter/Attack Aircraft Concepts," AIAA Paper 81-1675, AIAA Aircraft Systems and Technology Conference, Dayton, Ohio, Aug. 11-13, 1981.

⁶Williams, T. L. and Hunt, B. L., "Top Inlet Feasibility for Transonic-Supersonic Fighter Aircraft Applications," AIAA Paper 80-1809, AIAA Aircraft Systems Meeting, Anaheim, Calif., 1980.

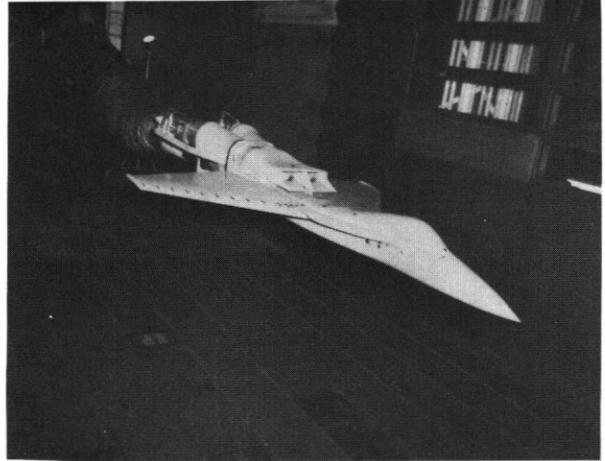
⁷Williams, T. L., Nelms, W. P. and Smeltzer, D. B., "Top-Mounted Inlet System Feasibility for Transonic-Supersonic Fighter Aircraft," AGARD Paper, AGARD Symposium on Aerodynamics of Power Plant Installation, Toulouse, France, May 11-14, 1981.

⁸Smeltzer, D. B., Nelms, W. P. and Williams, T. L., "Airframe Effects on a Top-Mounted Inlet System for V/STOL Fighter Aircraft," AIAA Paper 81-2631, AIAA/NASA-Ames V/STOL Conference, Palo Alto, Calif., 1981.

⁹Frink, N. T. and Lamar, J. E., "Water-Tunnel and Analytical Investigation of the Effect of Strake Design Variables on Strake Vortex Breakdown Characteristics," NASA TP-1676, 1980.



Force Model



Inlet-Pressure Model

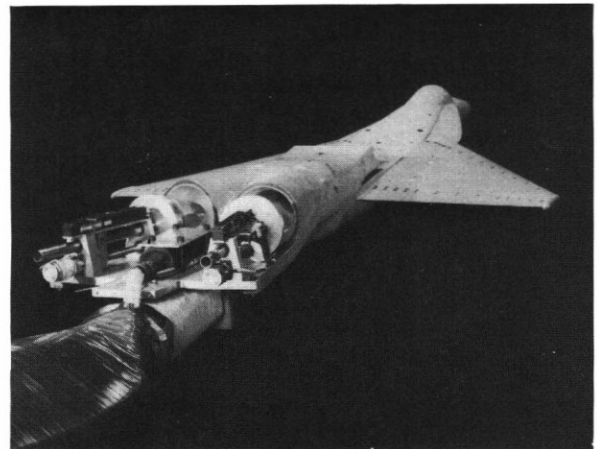
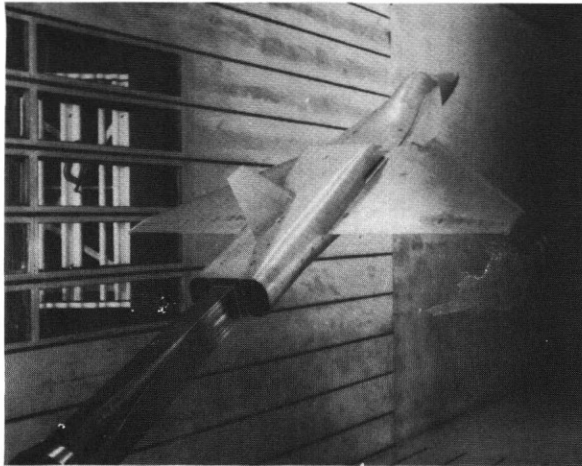


Fig. 1 Force and inlet-pressure models installed in the 11- by 11-foot Transonic Wind Tunnel.

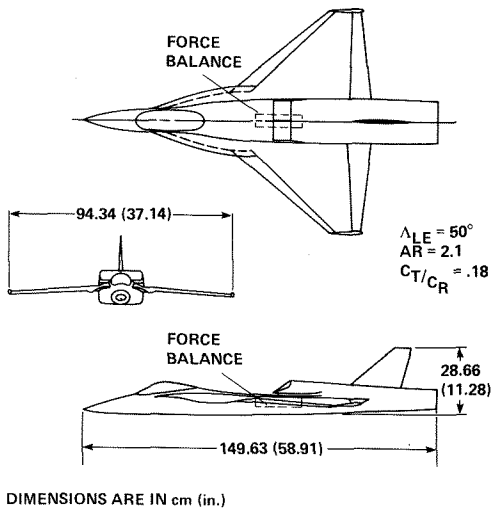


Fig. 2 Force model.

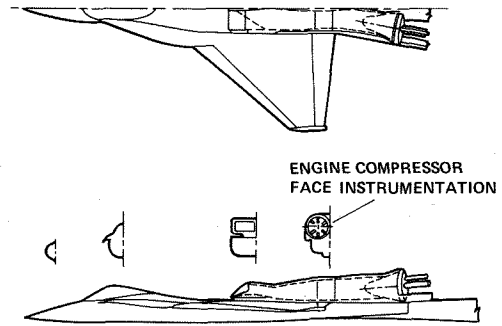


Fig. 3 Inlet-pressure model.

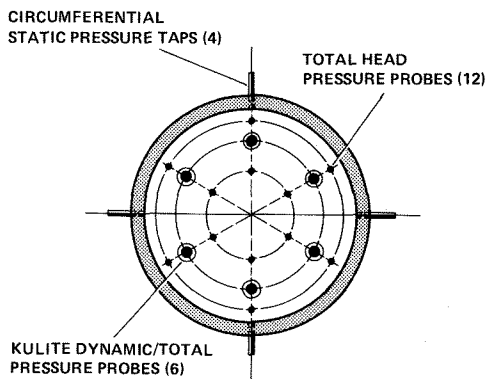


Fig. 4 Compressor face instrumentation.

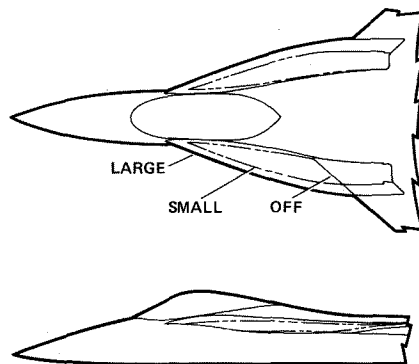


Fig. 5 Leading-edge extension (LEX) options.

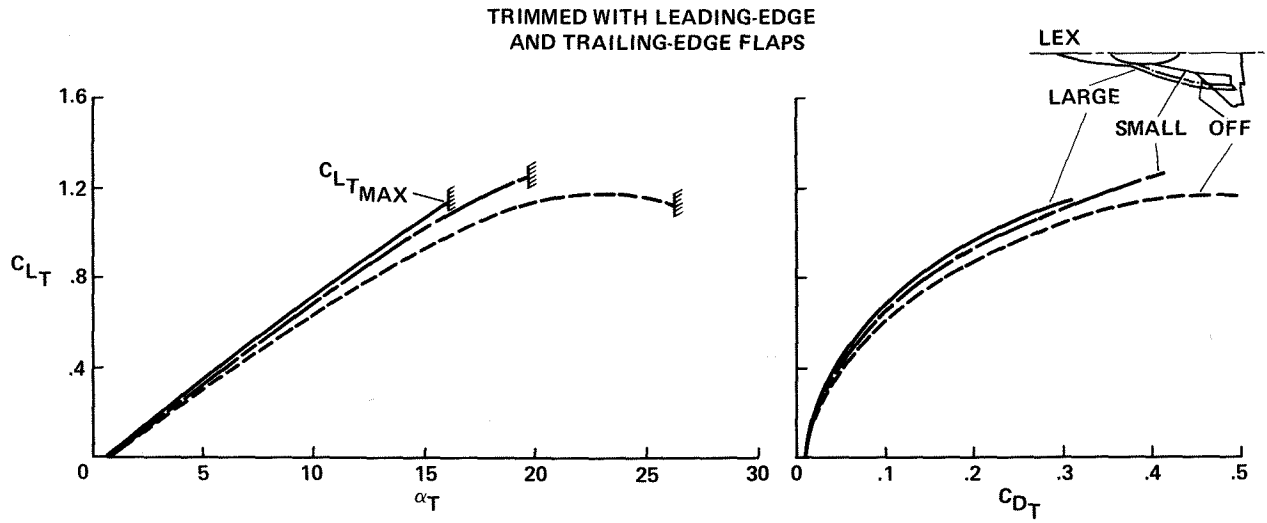


Fig. 6 Trimmed lift and drag: $M = 0.6$.

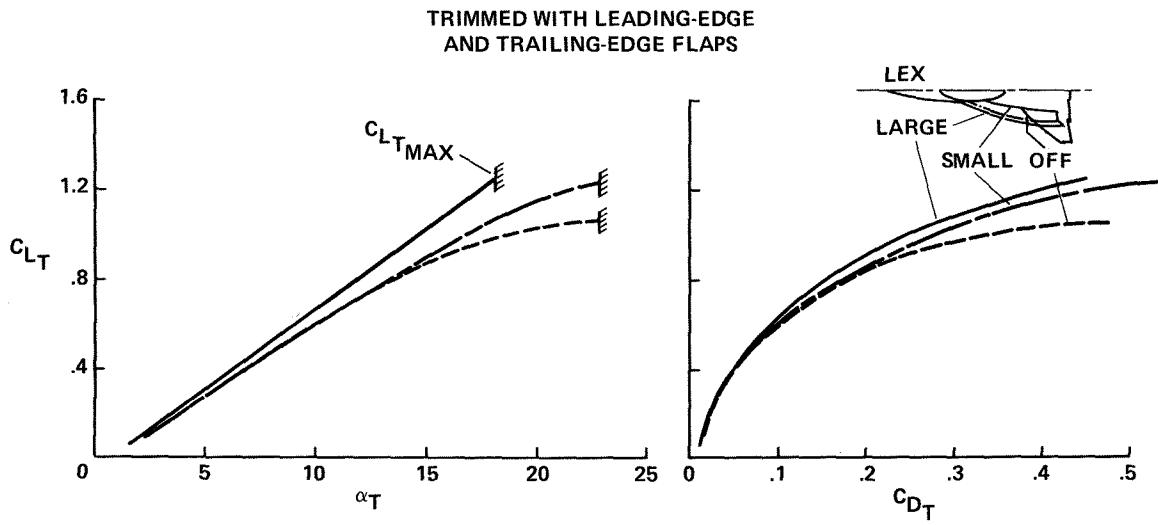


Fig. 7 Trimmed lift and drag: $M = 0.9$.

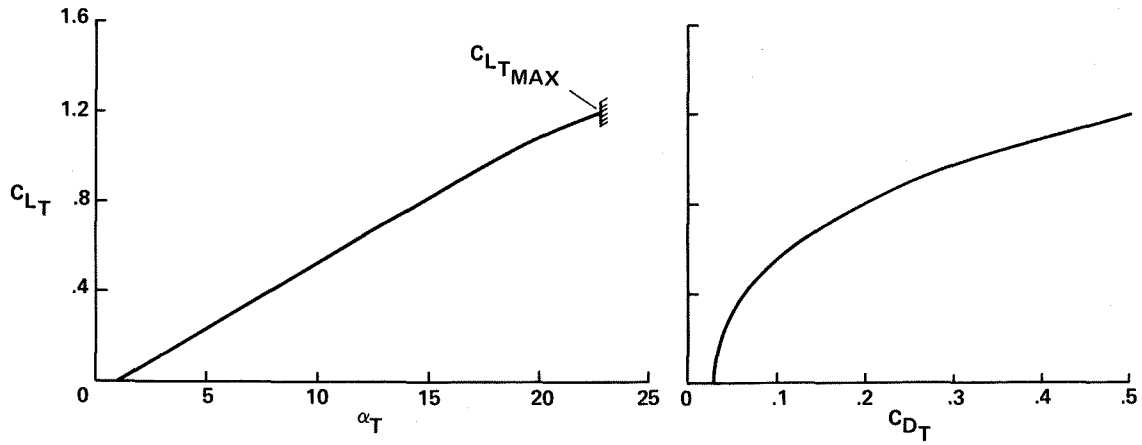


Fig. 8 Trimmed lift and drag: $M = 1.2$.

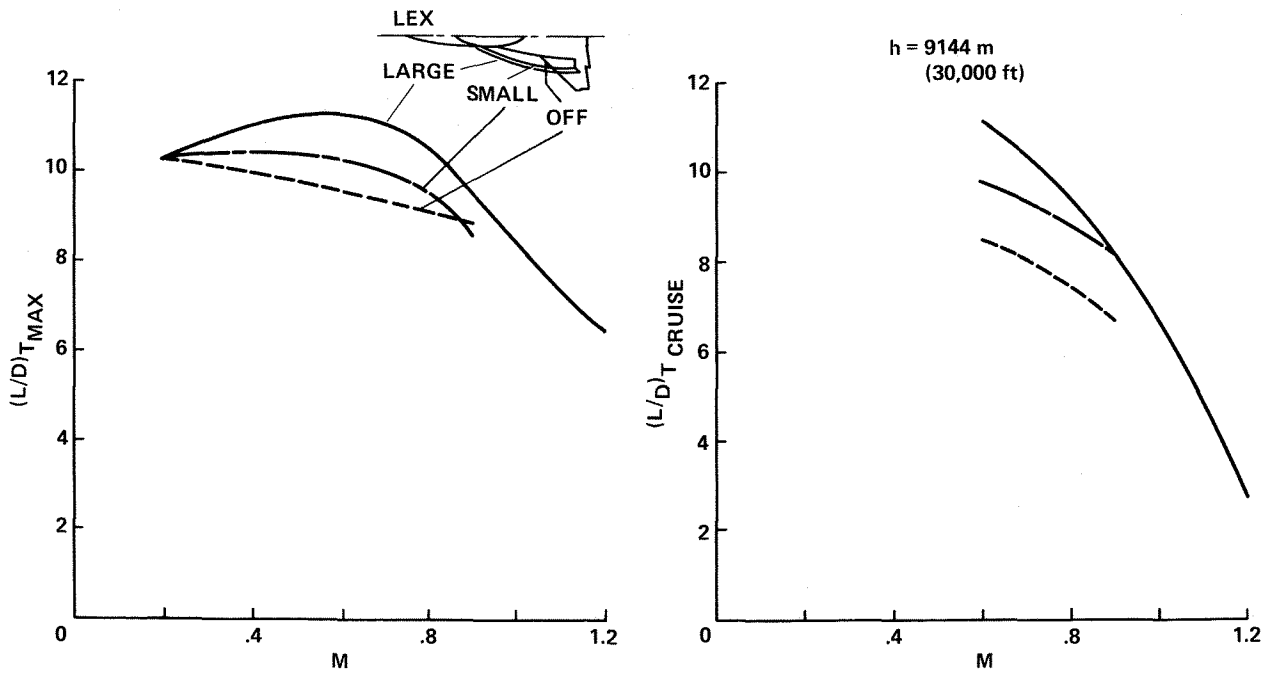


Fig. 9 Trimmed lift-to-drag ratio summaries: a) $(L/D)_{T_{max}}$; b) $(L/D)_{T_{cruise}}$

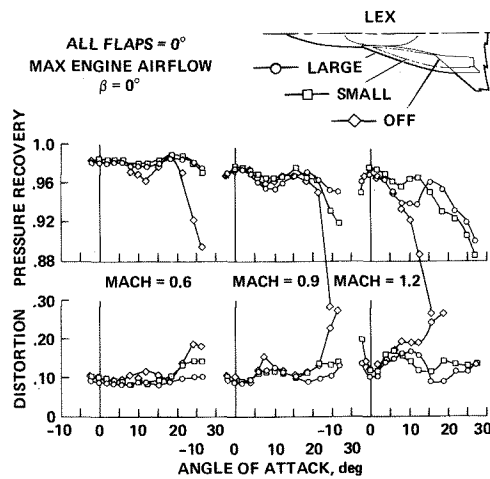


Fig. 10 LEX size effects on inlet-pressure recovery and distortion.

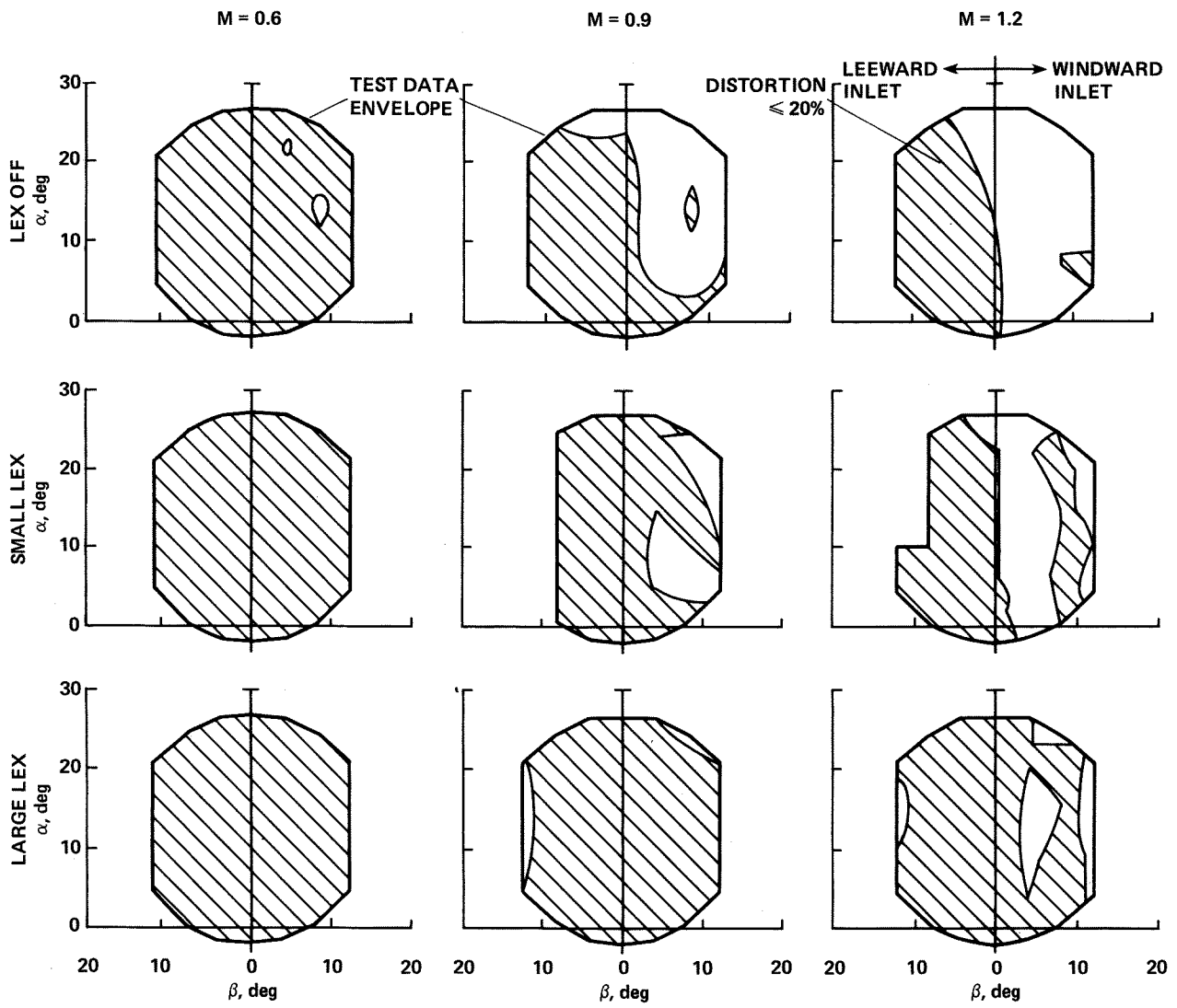


Fig. 11 Distortion-limited operating envelopes.

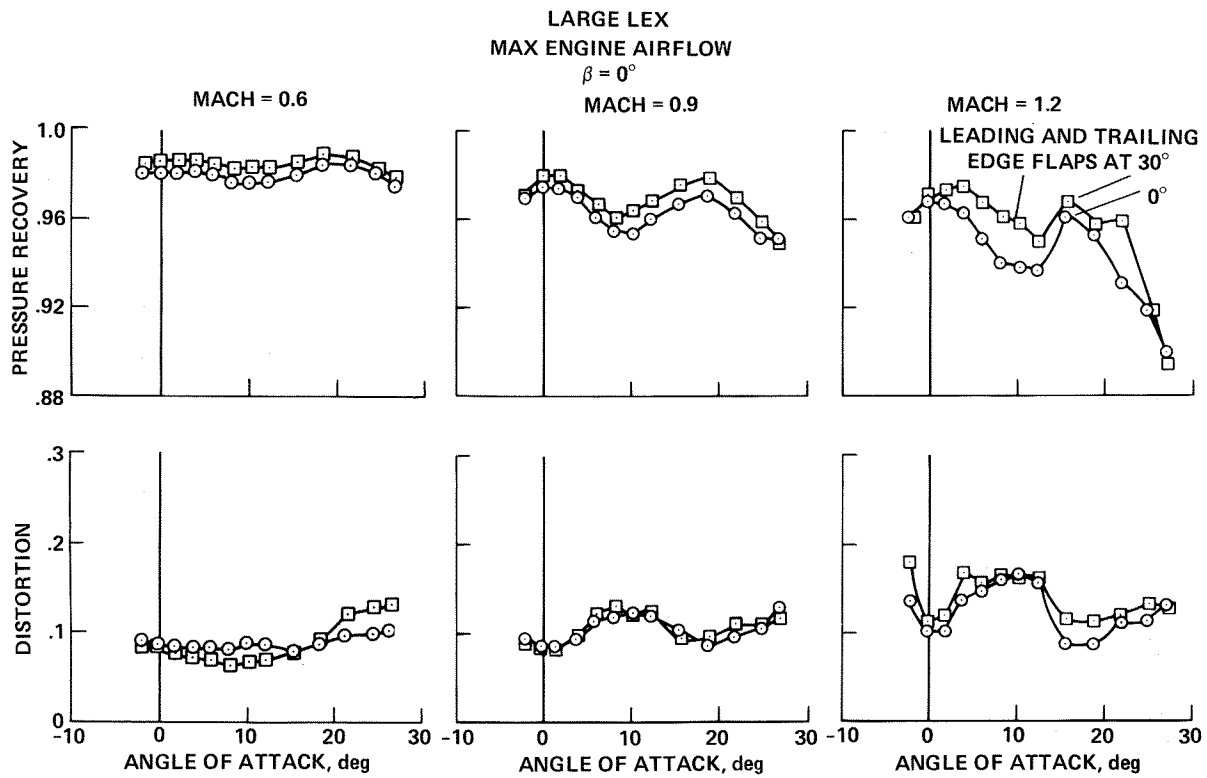


Fig. 12 Flap-deflection effects on inlet-pressure recovery and distortion.

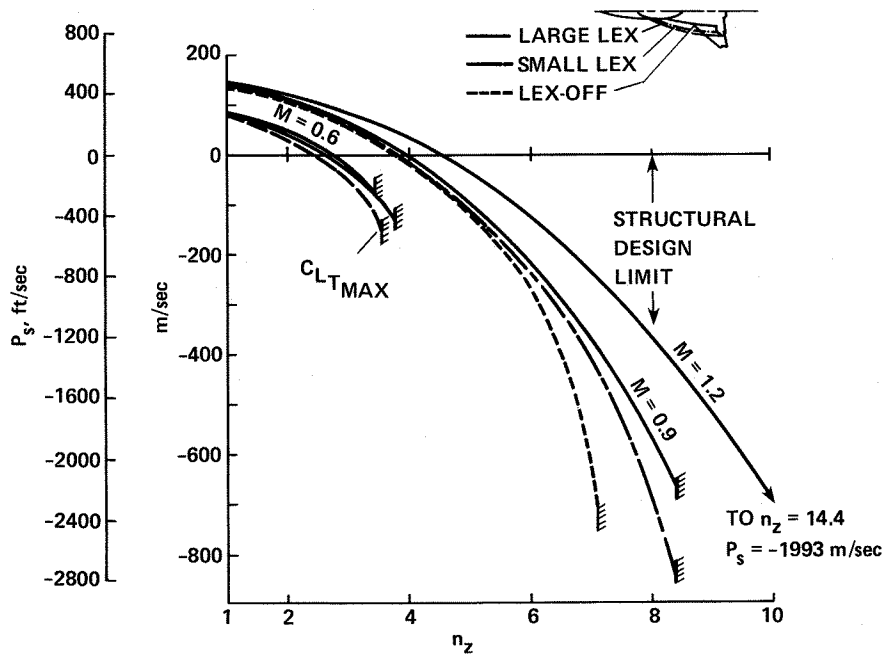


Fig. 13 Airplane maneuver performance.